




## RESEARCH ARTICLE

# Changes in white matter fiber density and morphology across the adult lifespan: A cross-sectional fixel-based analysis

Shao Wei Choy<sup>1</sup>  | Epifanio Bagarinao<sup>2</sup>  | Hirohisa Watanabe<sup>2,3,4</sup> | Eric Tatt Wei Ho<sup>1</sup> | Satoshi Maesawa<sup>2,5</sup> | Daisuke Mori<sup>2</sup> | Kazuhiro Hara<sup>4</sup> | Kazuya Kawabata<sup>4</sup> | Noritaka Yoneyama<sup>4</sup> | Reiko Ohdake<sup>4</sup> | Kazunori Imai<sup>4</sup> | Michihito Masuda<sup>4</sup> | Takamasa Yokoi<sup>4</sup> | Aya Ogura<sup>4</sup> | Toshiaki Taoka<sup>6</sup> | Shuji Koyama<sup>2</sup> | Hiroki C. Tanabe<sup>7</sup> | Masahisa Katsuno<sup>4</sup> | Toshihiko Wakabayashi<sup>5</sup> | Masafumi Kuzuya<sup>8</sup> | Minoru Hoshiyama<sup>2</sup> | Haruo Isoda<sup>2</sup> | Shinji Naganawa<sup>6</sup> | Norio Ozaki<sup>2,9</sup> | Gen Sobue<sup>2</sup> 

<sup>1</sup>Center for Intelligent Signal and Imaging Research, Universiti Teknologi Petronas, Seri Iskandar, Perak, Malaysia

<sup>2</sup>Brain and Mind Research Center, Nagoya University, Nagoya, Aichi, Japan

<sup>3</sup>Department of Neurology, Fujita Health University School of Medicine, Toyoake, Aichi, Japan

<sup>4</sup>Department of Neurology, Nagoya University Graduate School of Medicine, Nagoya, Aichi, Japan

<sup>5</sup>Department of Neurosurgery, Nagoya University Graduate School of Medicine, Nagoya, Aichi, Japan

<sup>6</sup>Department of Radiology, Nagoya University Graduate School of Medicine, Nagoya, Aichi, Japan

<sup>7</sup>Department of Cognitive and Psychological Sciences, Graduate School of Informatics, Nagoya University, Nagoya, Aichi, Japan

<sup>8</sup>Department of Community Healthcare and Geriatrics, Nagoya University Graduate School of Medicine and Institute of Innovation for Future Society, Nagoya University, Nagoya, Aichi, Japan

<sup>9</sup>Department of Psychiatry, Nagoya University Graduate School of Medicine, Nagoya, Aichi, Japan

## Correspondence

Gen Sobue, Brain and Mind Research Center, Nagoya University Graduate School of Medicine, 65 Tsurumai-cho, Showa-ku, Nagoya, Aichi 466-8550 Japan.  
Email: sobueg@med.nagoya-u.ac.jp

## Funding information

Ministry of Education, Culture, Sports, Science and Technology, Grant/Award Numbers: 26117002, 80569781; Ministry of Health, Labour and Welfare; Ministry of Higher Education Malaysia HI-CoE Program

## Abstract

White matter (WM) fiber bundles change dynamically with age. These changes could be driven by alterations in axonal diameter, axonal density, and myelin content. In this study, we applied a novel fixel-based analysis (FBA) framework to examine these changes throughout the adult lifespan. Using diffusion-weighted images from a cohort of 293 healthy volunteers (89 males/204 females) from ages 21 to 86 years old, we performed FBA to analyze age-related changes in microscopic fiber density (FD) and macroscopic fiber morphology (fiber cross section [FC]). Our results showed significant and widespread age-related alterations in FD and FC across the whole brain. Interestingly, some fiber bundles such as the anterior thalamic radiation, corpus callosum, and superior longitudinal fasciculus only showed significant negative relationship with age in FD values, but not in FC. On the other hand, some segments of the cerebello-thalamo-cortical pathway only showed significant negative relationship with age in FC, but not in FD. Analysis at the tract-level also showed that major fiber tract groups predominantly distributed in the frontal lobe (cingulum, forceps minor)

This is an open access article under the terms of the Creative Commons Attribution-NonCommercial License, which permits use, distribution and reproduction in any medium, provided the original work is properly cited and is not used for commercial purposes.

© 2020 The Authors. *Human Brain Mapping* published by Wiley Periodicals, Inc.

exhibited greater vulnerability to the aging process than the others. Differences in FC and the combined measure of FD and cross section values observed between sexes were mostly driven by differences in brain sizes although male participants tended to exhibit steeper negative linear relationship with age in FD as compared to female participants. Overall, these findings provide further insights into the structural changes the brain's WM undergoes due to the aging process.

#### KEYWORDS

adult lifespan, aging, fiber cross section, fiber density, fixel-based analysis, white matter

## 1 | INTRODUCTION

Healthy aging is characterized by changes in brain structure and function. Studies using magnetic resonance imaging (MRI) have consistently shown age-related increase in the volume of cerebrospinal fluid (CSF; Good et al., 2001; Smith, Chebrolu, Wekstein, Schmitt, & Markesbery, 2007), decline in the global gray matter (GM) volume (Allen, Bruss, Brown, & Damasio, 2005; Bagarinao et al., 2018; Good et al., 2001; Smith et al., 2007) and no changes in white matter (WM) volume (Good et al., 2001; Smith et al., 2007; Taki et al., 2004). A few studies, however, reported WM volume decreases with age (Greenberg et al., 2008; Jernigan et al., 2001) or age-related alterations characterized by a nonlinear relationship where an initial increase in WM volume is followed by an accelerated decline in old age (Bagarinao et al., 2018; Fjell et al., 2013; Ryali, Glover, Chang, & Menon, 2009; Taki et al., 2011). Volumetric characterization of age-related WM changes is incomplete as alterations in WM tracts can also occur even without detectable changes in WM volume.

With advances in diffusion weighted imaging (DWI), examination of the microstructural changes associated with age in WM fiber tracts has become possible. DWI can be used to evaluate the microscopic diffusion of water molecules in various brain tissues. Due to the presence of axonal membranes and myelin sheaths in WM, water molecules preferentially diffused in the direction parallel to the long axis of the axonal bundles. Thus, measures associated with the rate (e.g., mean diffusivity [MD]) and directionality (fractional anisotropy [FA]) of water diffusion can be used as indirect measures of WM integrity. The association between diffusion parameters and WM fiber properties has been demonstrated in animal studies (Song et al., 2003; Song et al., 2005; Takahashi et al., 2002). For instance, measures associated with the rate of diffusion along the primary axis of the diffusion ellipsoid, called axial diffusivity (AD), had been shown to be sensitive to axonal differences, whereas that in the secondary axis, called radial diffusivity (RD), is sensitive to myelin changes (Song et al., 2003; Song et al., 2005). Using these measures, several studies have investigated age-related changes in WM integrity (Bennett & Madden, 2014; Cox et al., 2016; Lebel et al., 2012; Sala et al., 2012; Salat et al., 2005; Sullivan & Pfefferbaum, 2006). Generally, FA had been shown to decrease with age while MD had been shown to increase, an indication of the general decline in WM integrity in healthy aging (Cox et al., 2016; Hsu et al., 2010; Inano, Takao,

Hayashi, Abe, & Ohtomo, 2011). This age-related decline in WM integrity was also shown to vary considerably across brain regions and likely driven by changes in the underlying myelin as evidenced by the preferential increases in RD as compared to AD (Inano et al., 2011; Kumar, Chavez, Macey, Woo, & Harper, 2013).

These scalar indices, however, are indirect measures, not fiber-specific, and have poor interpretability. Estimation of these measures from DWI data is confounded in voxels where contributions from multiple fibers (the so-called crossing or kissing fibers) are present. The diffusion tensor model only performs well in regions where fibers are aligned in a single axis, but poorly in regions containing several distinct fiber populations with differing orientations. Specifically, it has not been able to directly elucidate the changes in WM as influenced by different biophysical properties including axon diameter, axon density, and myelin concentration, among others. To address these issues, a framework called fixel-based analysis (FBA) was recently proposed (Raffelt et al., 2017). This framework uses a more advanced diffusion MRI model that can resolve multiple fiber populations in a single voxel (Tournier, Mori, & Leemans, 2011), and thus enables the extraction of measures directly associated with a single fiber population in a given voxel called a fixel. Metrics extracted using FBA include fiber density (FD), fiber cross section (FC), and the combined measure of FD and cross section (FDC). FD estimates the microscopic density of neuronal axons within a fixel, while FC estimates the macroscopic change in the cross-sectional area perpendicular to the fiber bundle experienced during template registration.

Recently, Genc et al. (2018) used FBA to examine age-related changes in WM FD and morphology over childhood. They found statistically significant increases in FD over time localized to medial and posterior commissural and association fibers, while increases in FC were substantially more extensive. Other studies have also used FBA to examine WM degeneration in older clinical populations including multiple sclerosis (Gajamange et al., 2018) and Alzheimer's disease (Mito et al., 2018). However, investigations of age-related WM alterations covering adulthood, the majority of the human lifespan, have not yet been reported in the literature. In this study, we used FBA to comprehensively investigate age-related changes in FD, FC, and FDC. These quantities relate to the capacity of WM to transmit information, critical in brain function, and are therefore relevant in understanding the aging brain. We used DWI data from a cohort of 293 healthy

volunteers with age ranging from 21 to 86 years and examined age-related alterations in these measures across the adult lifespan.

## 2 | METHODS

### 2.1 | Participants

Data from 293 healthy volunteers with age ranging from 21 to 86 years old who participated in our on-going Brain and Mind Research Center Aging Cohort Study (Bagarinao et al., 2018; Bagarinao et al., 2019) were used in the analysis. Participants were recruited from Nagoya City and neighboring areas from July 2014 to March 2016. A total of 445 healthy adult participants were enrolled within this period. Participants were clinically assessed for general

cognitive performance using the Mini-Mental State Examination (MMSE) and the Japanese version of Addenbrooke's Cognitive Examination-Revised (ACE-R) (dos Santos Kawata et al., 2012; Mioshi, Dawson, Mitchell, Arnold, & Hodges, 2006) and for mood disturbances using the Beck Depression Inventory (Beck, Ward, Mendelson, Mock, & Erbaugh, 1961) by Japanese board-certified neurologists (H. W., K. H.) and neurosurgeon (S. M.). Of the 445 initially recruited, 152 participants were excluded due to (a) the participants' inability to complete the ACE-R (six participants), (b) structural abnormalities in magnetic resonance images (e.g., asymptomatic cerebral infarction, benign brain tumor, WM abnormalities, etc.; 128 participants), (c) MMSE score less than 26 or ACE-R total score less than 89 (16 participants), and (d) incomplete data (two participants). A summary of the participants' demographics and clinical characteristics is given in Table 1. All participants provided written informed consent before

**TABLE 1** Participants' characteristics

		All (n = 293)		Male (n = 89)		Female (n = 204)	
		Mean	SD	Mean	SD	Mean	SD
All	Age (years)	53.4	17.4	48.4	19.2	55.5	16.1
	MMSE	29.5	0.8	29.6	0.7	29.5	0.9
	ACE-R total	96.5	2.6	96.7	2.6	96.4	2.7
	Attention	17.9	0.3	17.9	0.3	17.9	0.3
	Memory	24.1	1.8	24.4	1.6	24.0	1.8
	Fluency	13.6	0.9	13.6	1.0	13.7	0.8
	Language	25.1	1.0	25.2	0.9	25.1	1.0
	Visuospatial	15.7	0.7	15.6	0.8	15.7	0.6
20s	Age (years)	24.3	2.6 (n = 47)	24.1	2.1 (n = 23)	24.5	3.0 (n = 24)
	MMSE	29.9	0.4	30.0	0.0	29.8	0.5
	ACE-R total	96.9	1.8	96.7	1.6	97.0	1.9
30s	Age (years)	33.4	2.8 (n = 28)	33.2	2.3 (n = 12)	33.6	3.1 (n = 16)
	MMSE	29.4	0.3	29.9	0.3	29.9	0.3
	ACE-R total	97.9	2.1	98.2	1.8	97.7	2.3
40s	Age (years)	44.7	3.1 (n = 26)	43.9	3.2 (n = 9)	45.1	2.9 (n = 17)
	MMSE	29.7	0.4	29.8	0.4	29.7	0.5
	ACE-R total	97.6	2.2	97.0	2.4	97.9	1.9
50s	Age (years)	54.7	3.1 (n = 52)	54.7	3.3 (n = 9)	54.7	3.0 (n = 43)
	MMSE	29.6	0.6	29.7	0.5	29.6	0.6
	ACE-R total	97.3	2.2	96.8	2.5	97.4	2.1
60s	Age (years)	64.9	2.6 (n = 81)	65.6	2.5 (n = 19)	64.6	2.6 (n = 62)
	MMSE	29.3	0.9	29.3	0.8	29.3	0.9
	ACE-R total	96.2	2.8	96.5	2.9	96.1	2.7
70s	Age (years)	72.3	2.4 (n = 56)	71.9	2.4 (n = 17)	72.5	2.4 (n = 39)
	MMSE	29.1	1.1	29.0	1.1	29.1	1.1
	ACE-R total	95.1	2.9	95.9	3.2	94.8	2.7
80s	Age (years)	83.7	1.7 (n = 3)	—	— (n = 0)	83.7	1.7 (n = 3)
	MMSE	29.0	0.8	—	—	29.0	0.8
	ACE-R total	91.3	1.2	—	—	91.3	1.2

Abbreviations: ACE-R, Addenbrooke's Cognitive Examination-Revised; MMSE, Mini-Mental State Examination; SD, standard deviation.

joining the study, which was reviewed and approved by the Ethics Committee of Nagoya University Graduate School of Medicine and conformed to the Ethical Guidelines for Medical and Health Research Involving Human Subjects as endorsed by the Japanese Government.

## 2.2 | Image acquisition

All participants were scanned at the Brain and Mind Research Center of Nagoya University using a 3 T Siemens Magnetom Verio (Siemens, Erlangen, Germany) system with a 32-channel head coil receiver. High resolution T1-weighted images were acquired from all participants using a 3D Magnetization Prepared Rapid Acquisition Gradient Echo (MPRAGE, Siemens) (Mugler & Brookeman, 1990) pulse sequence with the following imaging parameters: repetition time (TR)/MPRAGE TR = 7.4/2,500 ms, echo time (TE) = 2.48 ms, inversion time (TI) = 900 ms, 192 sagittal slices with a distance factor of 50% and 1-mm thickness, field of view (FOV) = 256 mm, 256 × 256 matrix dimension, in-plane voxel resolution of 1.0 × 1.0 mm, flip angle (FA) = 8°, and total scan time of 5 min and 49 s. DWIs were also acquired from all participants using the following imaging parameters: 80 axial slices with 2-mm slice thickness and distance factor of 0%, TR/TE = 13,600/92 ms, FOV = 196 mm, and 98 × 98 acquisition matrix. Voxel sizes were isotropic 2 mm in all dimensions. Sixty-four diffusion-weighted images ( $b = 1,000 \text{ s/mm}^2$ ) and one volume without diffusion weighting ( $b = 0 \text{ s/mm}^2$ ) were obtained with echo planar imaging. The DWI acquisition time is approximately 15 min and 26 s. Only single-phase encoded images were acquired for all participants.

## 2.3 | Total intracranial volume

The total intracranial volume (TIV) was computed using the acquired T1-weighted images. This was done by first segmenting the images into component images including GM, WM, and CSF, among others, using Statistical Parametric Mapping (SPM12; Wellcome Trust Center for Neuroimaging, London, UK) running on MATLAB (R2016a, MathWorks, Natick, MA). For each component image, the total volume was estimated by summing the volume of all the voxels surviving a threshold value equal to 0.2. TIV values were then computed as the sum of the total volumes of GM, WM, and CSF.

## 2.4 | FBA of DWI data

The acquired DWI data were processed using MRtrix3 (version 3.0, <http://www.mrtrix.org>) following the recommended FBA (Raffelt et al., 2017) preprocessing pipeline. We preprocessed the images to perform intensity normalization, denoising, Gibbs ringing removal, motion (Andersson & Sotiropoulos, 2016), and eddy current distortion correction (Smith et al., 2004). DWI data were upsampled to a  $1.3 \times 1.3 \times 1.3 \text{ mm}^3$  voxel resolution using the cubic interpolation

method included in the MRtrix3 package. Field inhomogeneities due to the EPI sequence remained uncorrected since we did not acquire reversed phase encoded images. We then computed the three-tissue response functions for WM, GM, and CSF using the *dhollander* algorithm in the *dwi2response* script, estimated the average across all participants, and generated voxel-wise fiber orientation distributions (FOD) by applying the multishell multitissue constrained spherical deconvolution (Jeurissen, Tournier, Dhollander, Connelly, & Sijbers, 2014) using only the average WM and CSF response functions on preprocessed images with a custom participant-specific whole-brain mask. To generate the individual whole-brain mask, we used the participant's T1-weighted image. The image was first segmented using *5ttgen* to extract the relevant component images, then coregistered to the upsampled  $b = 0$  DWI ( $b_0$ ) image using the Advanced Normalization Tools (ANTs, <http://stnava.github.io/ANTs/>) (Avants et al., 2014). The registered component images were then summed and thresholded to get an initial whole-brain mask. This mask was further refined using the Brain Extraction Tool, a component of the FSL software package (Jenkinson, Beckmann, Behrens, Woolrich, & Smith, 2012), to remove extraneous patches that remained after segmentation. We generated a second WM mask by combining the WM and subcortical tissue components, thresholding the resulting image using a value of 0.05, dilating the resulting mask using *maskfilter* ( $npass = 3$ ), and obtaining the intersection with the first whole-brain mask.

An unbiased study-specific population FOD template was generated using all participants' FOD data after performing a joint biased field and intensity normalization correction. Each participant's FOD was then registered to this template. A population template mask was also generated by computing the intersection of all the participants' WM masks in the template space. Using the population template mask, an analysis fixel mask was generated using a threshold value (*fmls\_peak\_value*) of 0.1. This value provided a good compromise between the inclusion of noisy fixels (e.g., crossing fixels in nearby GM regions) and the exclusion of genuine WM fixels especially in voxels containing crossing fibers. The normalized FODs were then segmented to estimate the fixels and the corresponding metrics including FD, FC, and FDC. Using the FOD template, whole brain tractography was also performed by synthesizing streamlines with the MRtrix probabilistic reconstruction algorithm using second order integration over FOD (iFOD2) (Tournier, Calamante, & Connelly, 2010). We generated 20 million streamlines with minimum length of 10 mm, maximum length of 250 mm, maximum angle between successive steps of 22.5°, and minimum FOD amplitude (cutoff) of 0.10. The generated tracts were further refined to 2 million streamlines using spherical-deconvolution informed filtering of tractograms (Smith, Tournier, Calamante, & Connelly, 2013). An outline of the full analysis scheme is depicted in Figure 1.

We used a general linear model (GLM) to identify significant associations between the different FBA metrics (FD, FC, and FDC) with age, sex, and TIV as covariates. The connectivity-based fixel enhancement method (Raffelt et al., 2015), part of the MRtrix3 software

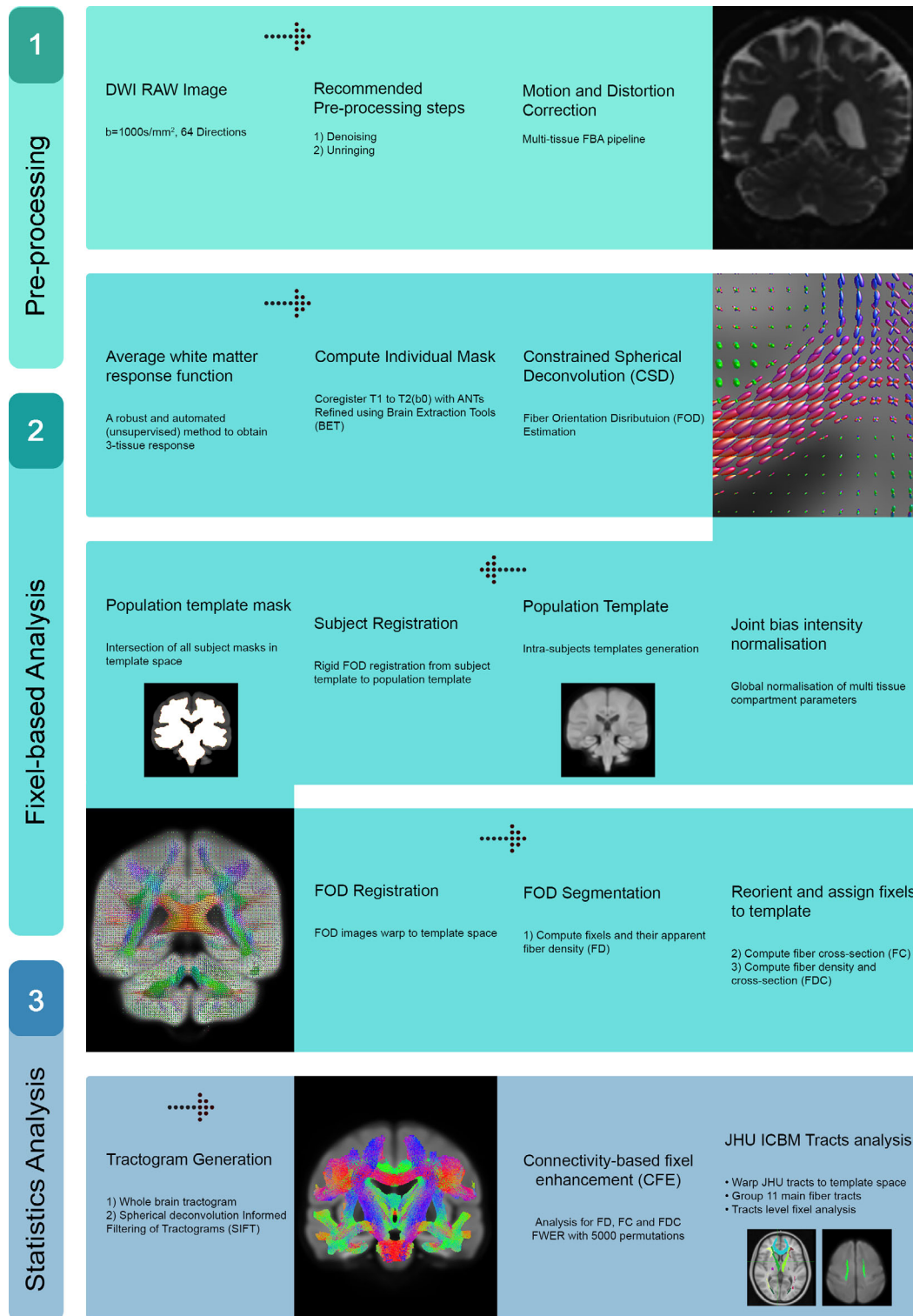


**FIGURE 1** Flowchart showing key steps of the cross-sectional fixel-based analysis framework used in this study

package, was used to estimate the relevant GLM parameters at the fixel level and the permutation-based, family wise error (FWE) corrected  $p$ -values of the computed parameters for each individual fixel in the template space. Statistical significance was assessed using 5,000 permutations and FWE-corrected  $p < .05$ .

### 2.5 | Tract-level analysis of FD, FC, and FDC

We also performed an analysis of the FBA metrics of the major fiber tracts. For this, we used the John Hopkins University (JHU) WM tractography atlas distributed with FSL to generate masks for 11 major

fiber tract groups (Hua et al., 2008) as shown in Figure 2. We normalized the JHU atlas into the population FOD template space using ANTs. Specifically, the upsampled b0 images were first normalized to the population template space and the mean image across all participants were computed. Using this mean image as the target image, we then registered the T2 image included in the JHU distribution using ANTs, obtained the relevant transformation information, and used this information to normalize the JHU tractography atlas. A mask for each tract group was then generated and the mean values of FD, FC, and FDC for all fixels within the mask were estimated. We used a linear regression model to identify the association between the mean values of FD, FC, and FDC across all fixels within each major tract and age. We used MATLAB (R2018b; MathWorks) for this analysis. For all regression analyses, sex and TIV were also included as regressors. Finally, FD, FC, and FDC values were also separately analyzed for each sex group by fitting a linear model using MATLAB with age and TIV as regressors. Statistical significance was corrected for multiple comparisons using a false discovery rate (FDR) of  $q < 0.05$ .

### 3 | RESULTS

#### 3.1 | Age-related changes of FBA metrics at the fixel level

Results of the GLM analyses at the fixel level showed widespread significant (FWE-corrected  $p < .05$ ) negative relationship between

age and FBA metrics across the whole brain (Figure 3, Supplementary Figures S1 and S2). Interestingly, some fiber bundles only showed significant negative association with age in FD, but not in FC. Examples include the corpus callosum, anterior thalamic radiation, and superior longitudinal fasciculus. On the other hand, fiber bundles in the cingulum of the cingulate gyrus and in the cerebello-thalamo-cortical pathway mainly showed significant negative relationship with age in FC, but not in FD.

#### 3.2 | Relationship of FBA metrics along major fiber tracts with age

Mean values of FD, FC, and FDC across all fixels within some major tracts showed significant (FDR  $q < 0.05$ ) negative linear relationship with age (Figures 4–6, Table 2). The mean FD values of the anterior thalamic radiation, cingulum of the cingulate gyrus and of the hippocampus, forceps minor, and superior longitudinal fasciculus were negatively associated with age. On the other hand, the mean log FC values of the cingulum of the cingulate gyrus, corticospinal tract, forceps minor, inferior fronto-occipital fasciculus, and inferior longitudinal fasciculus showed significant negative relationship with age, whereas that of the cingulum of the hippocampus showed positive relationship. In terms of FDC, fiber bundles in the anterior thalamic radiation, cingulum of the cingulate gyrus, corticospinal tract, forceps minor, inferior fronto-occipital fasciculus, and inferior longitudinal fasciculus showed significant negative linear relationship with

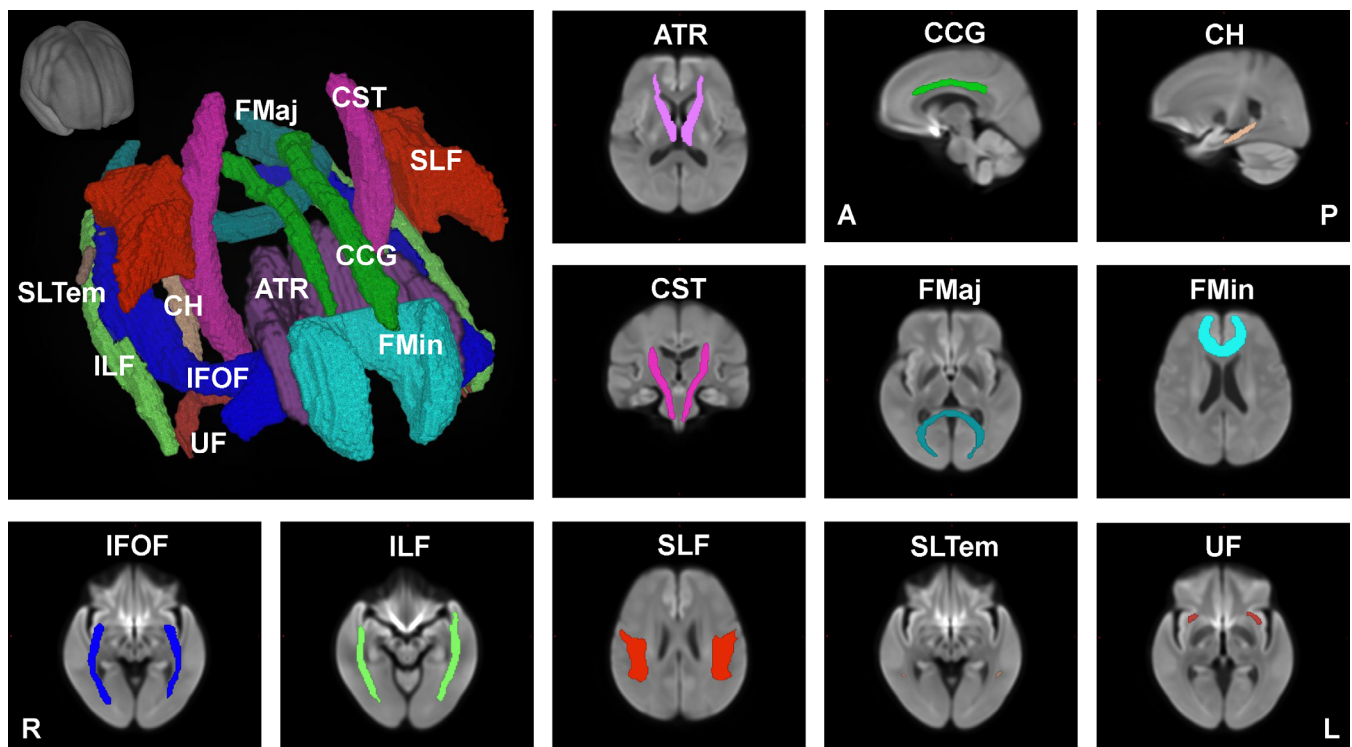


**FIGURE 2** Major fiber tracts from the John Hopkins University – International Consortium for Brain Mapping (JHU-ICBM) atlas warped into the study's population template space used for the tract-level analyses of FD, FC, and FDC. FC, fiber cross section; FD, fiber density; FDC, FD and cross section

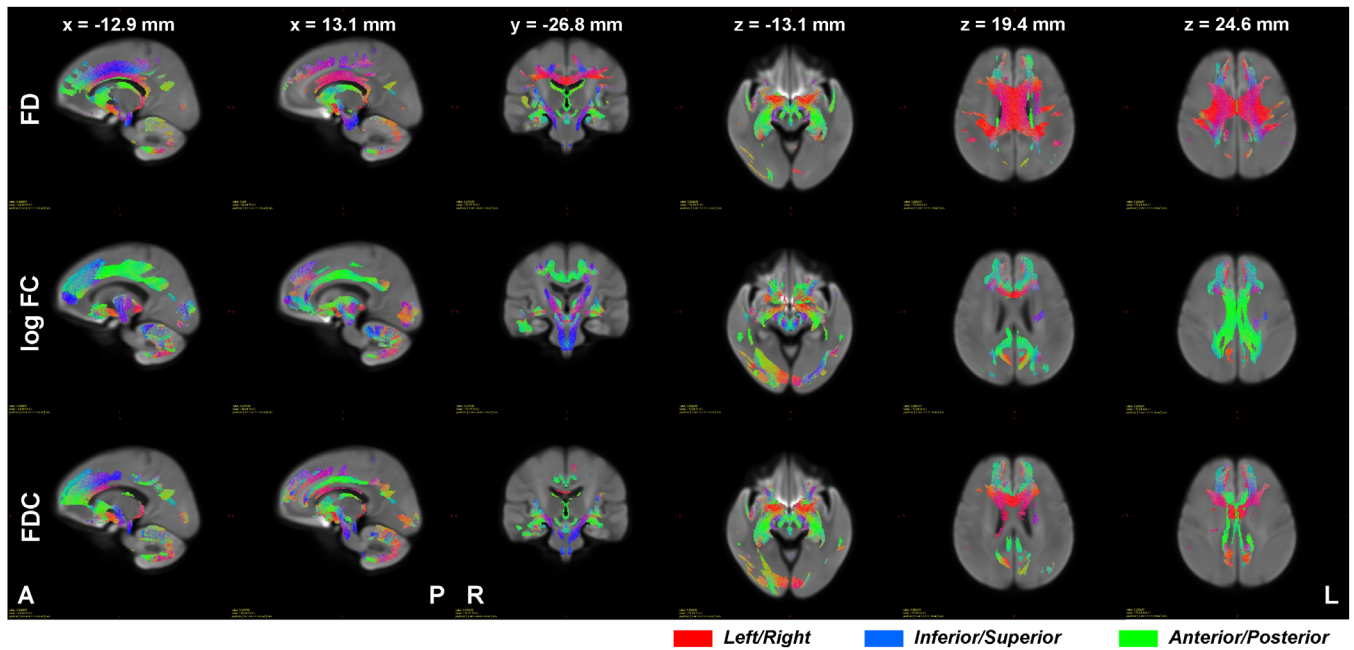


**FIGURE 3** Streamlines where significant (family wise error [FWE]-corrected  $p < .05$ ) negative relationship between FD (top row), log FC (middle row), and FDC (bottom row) and age were observed. Color encodes fiber direction with red for left–right, blue for inferior–superior, and green for anterior–posterior axes. Images are presented using radiological convention where the left hemisphere of the brain is shown at the right side of the image. A, anterior; FC, fiber cross section; FD, fiber density; FDC, FD and cross section; L, left; P, posterior; R, right

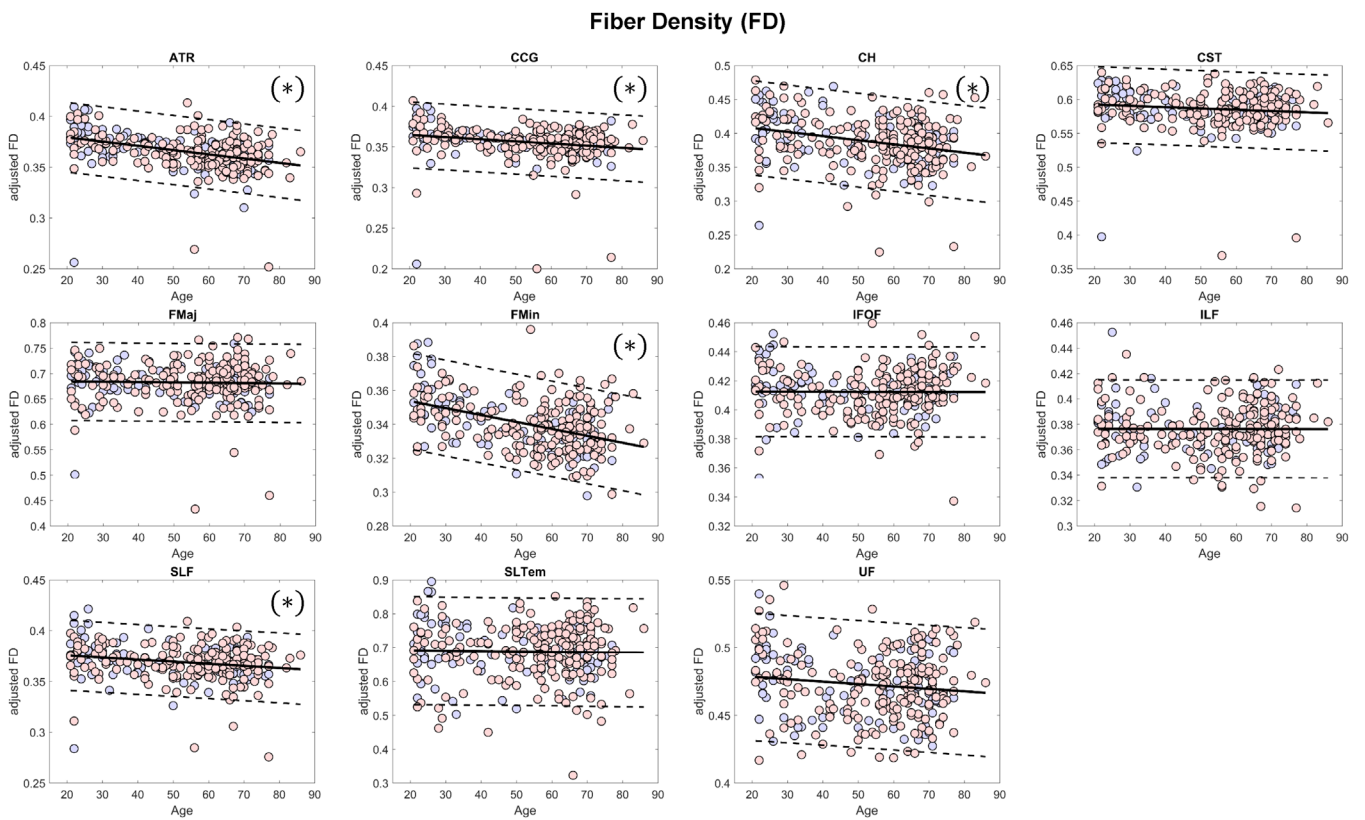


**FIGURE 4** Scatterplots (blue for male and red for female) of the mean FD values of the major fiber tract groups included in the analysis. Solid lines represent regression lines while dashed lines show 95% confidence interval. (\*)—indicates significant relationship with age (false discovery rate [FDR]  $q < 0.05$ ); ATR, anterior thalamic radiation; CCG, cingulum (cingulate gyrus); CH, cingulum (hippocampus); CST, corticospinal tract; FD, fiber density; FMaj, forceps major; FMin, forceps minor; IFOF, inferior fronto-occipital fasciculus; ILF, inferior longitudinal fasciculus; SLF, superior longitudinal fasciculus; SLTem, superior longitudinal fasciculus (temporal); UF, uncinate fasciculus

## Fiber Cross Section (FC)

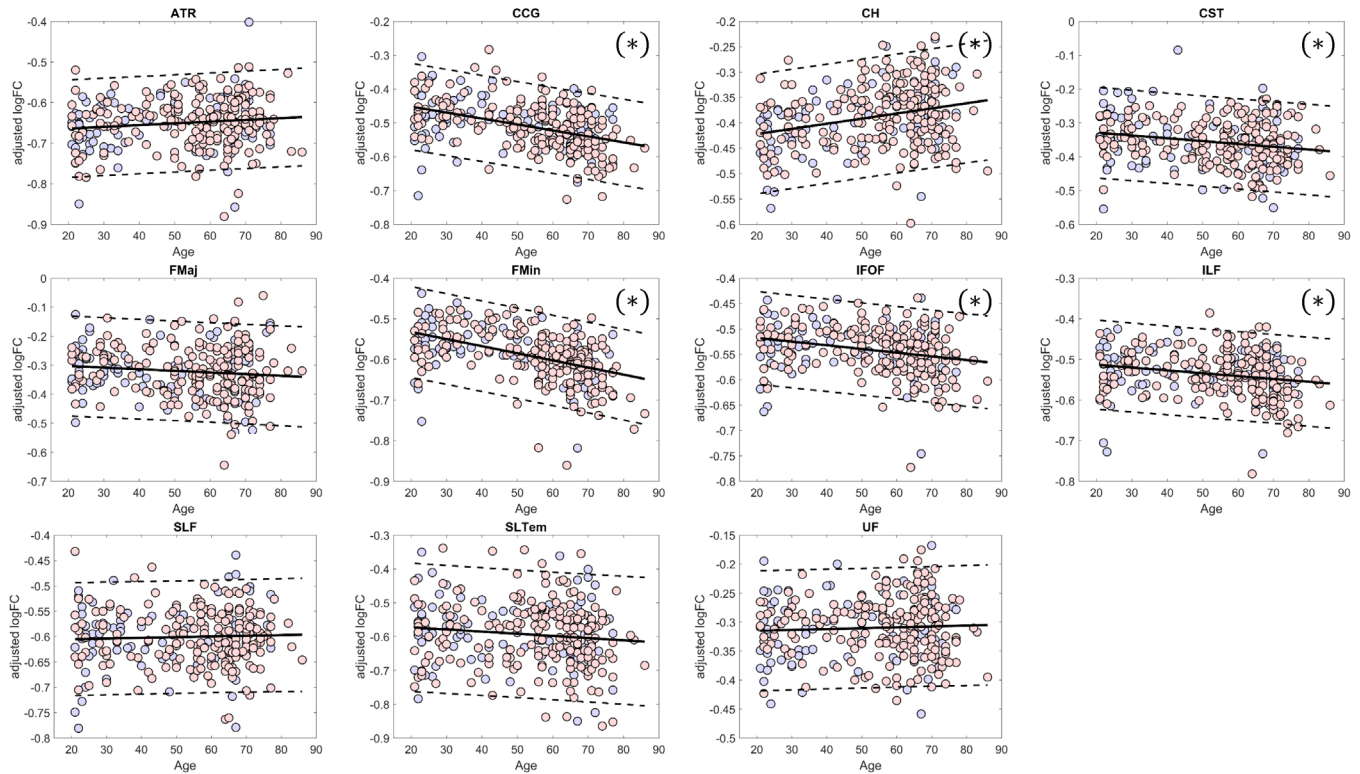


**FIGURE 5** Scatterplots (blue for male and red for female) of the mean log FC values of the major fiber tract groups included in the analysis. Solid lines represent regression lines while dashed lines show 95% confidence interval. (\*)—indicates significant relationship with age (false discovery rate [FDR]  $q < 0.05$ ); ATR, anterior thalamic radiation; CCG, cingulum (cingulate gyrus); CH, cingulum (hippocampus); CST, corticospinal tract; FC, fiber cross section; FMaj, forceps major; FMin, forceps minor; IFOF, inferior fronto-occipital fasciculus; ILF, inferior longitudinal fasciculus; SLF, superior longitudinal fasciculus; SLTem, superior longitudinal fasciculus (temporal); UF, uncinate fasciculus

age. Although many of the major fiber tract groups showed negative association with age in both FD and FC, subcortical fiber bundles in the anterior thalamic radiation and the cingulum (hippocampus) showed a different phenotype with lower FD but higher FC in the aged brain.

### 3.3 | Relationship with sex and TIV

We found no significant relationship between mean FC and FDC values and sex in all major fiber tracts examined except in the inferior longitudinal fasciculus for FDC (Table 2). Between mean FD values and sex, no significant association was observed in most major fiber tracts except in the anterior thalamic radiation and cingulum of the hippocampus (Table 2). On the other hand, TIV showed significant (FDR  $q < 0.05$ ) positive relationship with mean FC and FDC values in all fiber tract groups, whereas significant (FDR  $q < 0.05$ ) negative relationship with mean FD values was observed in the anterior thalamic radiation, cingulum of the cingulate gyrus, corticospinal tract, forceps major, superior longitudinal fasciculus, and uncinate fasciculus.

### 3.4 | Sex-specific changes in FBA metrics with age and TIV

Due to the unbalance number of participants between sexes in our cohort, we also performed separate analyses for each sex group. In male participants, we found significant (FDR  $q < 0.05$ ) negative linear relationship between mean FD values and age in the anterior thalamic radiation, cingulum of the hippocampus, forceps minor, and superior longitudinal fasciculus. Between mean FC values and age, significant (FDR  $q < 0.05$ ) negative relationship was observed in the cingulum of the cingulate gyrus and forceps minor, whereas positive relationship was observed in the cingulum of the hippocampus. Between mean FDC values and age, significant (FDR  $q < 0.05$ ) negative association was observed in the cingulum of the cingulate gyrus and forceps minor. Female participants showed the same behavior as that in all participants except in the superior longitudinal fasciculus in FD where the relationship was not significant. Males also tended to have lower (more negative) regression coefficient values associated with age in mean FD, whereas females had lower (more negative) coefficients in mean FC. Estimated values of the regression coefficients are summarized in Table 2.



## Fiber Density and Cross Section (FDC)

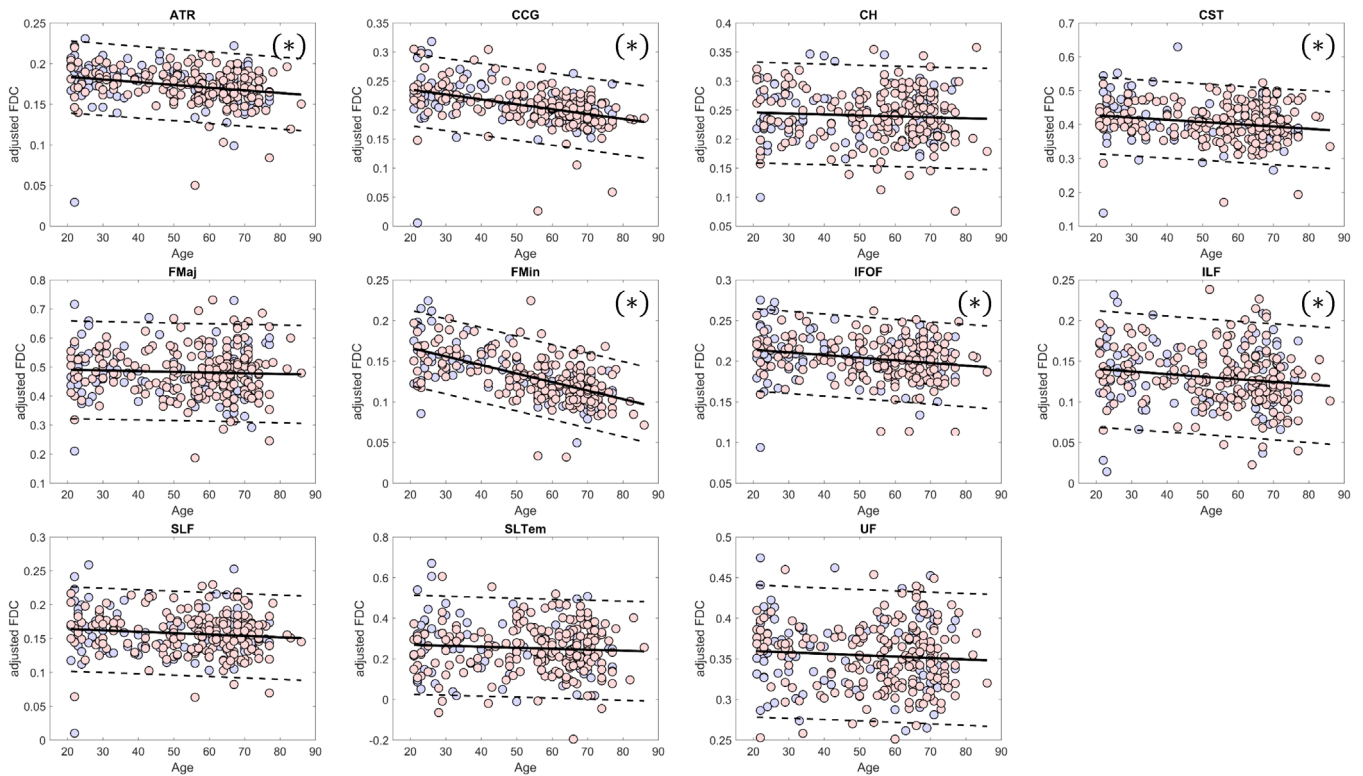


**FIGURE 6** Scatterplots (blue for male and red for female) of the mean FDC values of the major fiber tract groups included in the analysis. Solid lines represent regression lines while dashed lines show 95% confidence interval. (\*)—indicates significant relationship with age (false discovery rate [FDR]  $q < 0.05$ ); ATR, anterior thalamic radiation; CCG, cingulum (cingulate gyrus); CH, cingulum (hippocampus); CST, corticospinal tract; FD, fiber density; FDC, FD and cross section; FMaj, forceps major; FMin, forceps minor; IFOF, inferior fronto-occipital fasciculus; ILF, inferior longitudinal fasciculus; SLF, superior longitudinal fasciculus; SLTem, superior longitudinal fasciculus (temporal); UF, uncinat fasciculus

No significant relationship was observed between TIV and mean FD values in both groups. On the other hand, significant (FDR  $q < 0.05$ ) positive relationship was observed between TIV and mean FC and FDC values in both groups except in the corticospinal tract in FC and FDC in males and in the cingulum of the cingulate gyrus, forceps major, superior longitudinal fasciculus (temporal), and uncinat fasciculus in FDC also in males.

## 4 | DISCUSSION

This study examined fiber bundle density and fiber morphology (cross section) and how these measures are altered with age using FBA. First, we observed widespread age-related changes in FD and FC across the whole brain. The degree of the linear association between FBA metrics and age was not homogeneous across major fiber tract groups with some fiber tract groups exhibiting more vulnerability to aging process than others. This is particularly the case for fiber tract groups connecting to the frontal lobe including the cingulum of the cingulate gyrus and forceps minor which showed the two highest negative slopes of the linear relationship with age (in terms of FDC values) indicating significantly lower FD and FC values in the aging

brain. On the other hand, FC values of the corpus callosum fibers were relatively well preserved. Major fiber tract groups connecting to subcortical regions, namely the anterior thalamic radiation tract and the cingulum connecting to the hippocampus, had FC that even showed tendency to increase with age. Second, differences in FC and FDC values observed between sexes were mostly driven by differences in brain sizes although male participants tended to exhibit relatively lower (more negative) slopes in FD values with age as compared to female participants.

### 4.1 | Widespread cross-sectional changes in FD with aging

To the best of our knowledge, this is the first study to demonstrate the relationship between age and FD, FC, as well as FDC in the adult lifespan. Age-related microstructural changes in WM fiber tracts have been reported in the literature (Bennett & Madden, 2014; Cox et al., 2016; Lebel et al., 2012; Sala et al., 2012; Salat et al., 2005; Sullivan & Pfefferbaum, 2006). Using diffusion scalar indices, these studies have shown significant decreases in FA with age usually attributed to alterations in the underlying myelin as evidenced by the

**TABLE 2** Estimated values of the regression coefficients for the tract-level analyses

FBA metric	Tracts	All			Male		Female	
		Age	Sex	TIV	Age	TIV	Age	TIV
FD	ATR	<b>-4.19E-04</b>	<b>-9.13E-03</b>	<b>-2.84E-05</b>	<b>-4.46E-04</b>	-4.35E-05	<b>-4.01E-04</b>	-2.11E-05
	CCG	<b>-2.66E-04</b>	-5.94E-03	<b>-3.23E-05</b>	-2.64E-04	-4.85E-05	<b>-2.66E-04</b>	-2.45E-05
	CH	<b>-6.10E-04</b>	<b>1.82E-02</b>	-1.77E-05	<b>-7.04E-04</b>	6.61E-06	<b>-5.54E-04</b>	-2.91E-05
	CST	-1.90E-04	3.86E-03	<b>-3.61E-05</b>	-2.18E-04	-4.43E-05	-1.71E-04	-3.20E-05
	FMaj	-6.46E-05	-1.13E-02	<b>-4.67E-05</b>	-9.29E-05	-3.47E-05	-4.80E-05	-5.25E-05
	FMin	<b>-4.09E-04</b>	-4.35E-03	-1.02E-05	<b>-5.69E-04</b>	-6.93E-06	<b>-3.11E-04</b>	-1.12E-05
	IFOF	-3.92E-06	-2.51E-03	-1.33E-05	-1.08E-04	-1.69E-05	6.05E-05	-1.12E-05
	ILF	-3.73E-06	8.27E-03	8.14E-06	-6.23E-06	-5.58E-06	-1.27E-06	1.48E-05
	SLF	<b>-2.08E-04</b>	4.29E-05	<b>-2.22E-05</b>	<b>-3.20E-04</b>	-3.20E-05	-1.38E-04	-1.71E-05
	SLtem	-1.02E-04	1.05E-02	-7.52E-05	-7.44E-04	-1.32E-04	2.97E-04	-4.55E-05
	UF	-1.79E-04	-8.10E-03	<b>-3.03E-05</b>	-2.76E-04	-5.07E-05	-1.19E-04	-2.01E-05
logFC	ATR	4.31E-04	1.13E-03	<b>4.77E-04</b>	6.49E-04	<b>4.25E-04</b>	3.01E-04	<b>5.02E-04</b>
	CCG	<b>-1.76E-03</b>	-5.47E-03	<b>3.95E-04</b>	<b>-1.04E-03</b>	<b>3.12E-04</b>	<b>-2.20E-03</b>	<b>4.33E-04</b>
	CH	<b>1.01E-03</b>	-5.68E-03	<b>3.11E-04</b>	<b>1.52E-03</b>	<b>2.50E-04</b>	<b>6.98E-04</b>	<b>3.39E-04</b>
	CST	<b>-8.37E-04</b>	-6.37E-03	<b>2.69E-04</b>	-9.37E-04	1.50E-04	<b>-7.68E-04</b>	<b>3.26E-04</b>
	FMaj	-5.67E-04	-4.60E-03	<b>2.97E-04</b>	-4.61E-04	<b>2.81E-04</b>	-6.32E-04	<b>3.04E-04</b>
	FMin	<b>-1.75E-03</b>	1.66E-02	<b>4.71E-04</b>	<b>-1.32E-03</b>	<b>4.75E-04</b>	<b>-2.02E-03</b>	<b>4.68E-04</b>
	IFOF	<b>-7.28E-04</b>	1.09E-02	<b>4.06E-04</b>	-5.02E-04	<b>3.90E-04</b>	<b>-8.67E-04</b>	<b>4.13E-04</b>
	ILF	<b>-7.00E-04</b>	1.77E-02	<b>4.29E-04</b>	-1.42E-04	<b>3.48E-04</b>	<b>-1.04E-03</b>	<b>4.67E-04</b>
	SLF	1.33E-04	2.25E-02	<b>4.58E-04</b>	5.21E-04	<b>4.39E-04</b>	-1.04E-04	<b>4.65E-04</b>
	SLtem	-6.38E-04	4.37E-02	<b>4.96E-04</b>	-5.23E-04	<b>3.82E-04</b>	-7.01E-04	<b>5.51E-04</b>
	UF	1.52E-04	-2.03E-02	<b>2.84E-04</b>	3.80E-04	<b>2.48E-04</b>	1.45E-05	<b>3.00E-04</b>
FDC	ATR	<b>-3.33E-04</b>	-1.07E-02	<b>1.15E-04</b>	-3.16E-04	<b>8.98E-05</b>	<b>-3.42E-04</b>	<b>1.28E-04</b>
	CCG	<b>-8.43E-04</b>	-9.33E-03	<b>8.60E-05</b>	<b>-6.66E-04</b>	5.47E-05	<b>-9.49E-04</b>	<b>1.01E-04</b>
	CH	-1.67E-04	1.50E-02	<b>1.04E-04</b>	-8.79E-05	<b>1.09E-04</b>	-2.16E-04	<b>1.01E-04</b>
	CST	<b>-6.58E-04</b>	-1.75E-03	<b>1.02E-04</b>	-8.39E-04	4.63E-05	<b>-5.43E-04</b>	<b>1.30E-04</b>
	FMaj	-2.43E-04	-1.62E-02	<b>1.38E-04</b>	-2.83E-04	1.59E-04	-2.20E-04	<b>1.28E-04</b>
	FMin	<b>-1.05E-03</b>	2.01E-03	<b>1.52E-04</b>	<b>-1.18E-03</b>	<b>1.70E-04</b>	<b>-9.68E-04</b>	<b>1.44E-04</b>
	IFOF	<b>-3.25E-04</b>	6.46E-04	<b>1.46E-04</b>	-3.70E-04	<b>1.43E-04</b>	<b>-2.97E-04</b>	<b>1.48E-04</b>
	ILF	<b>-3.17E-04</b>	<b>1.85E-02</b>	<b>2.02E-04</b>	-1.05E-04	<b>1.58E-04</b>	<b>-4.45E-04</b>	<b>2.22E-04</b>
	SLF	-2.03E-04	8.18E-03	<b>1.40E-04</b>	-2.37E-04	<b>1.28E-04</b>	-1.82E-04	<b>1.46E-04</b>
	SLtem	-4.89E-04	4.51E-02	<b>2.78E-04</b>	-1.32E-03	1.37E-04	3.10E-05	<b>3.50E-04</b>
	UF	-1.74E-04	-1.85E-02	<b>8.43E-05</b>	-2.59E-04	5.08E-05	-1.19E-04	<b>1.01E-04</b>

Note: Values of the estimated regression coefficients in bold are significant (corrected for multiple comparisons using FDR  $q < 0.05$ ).

Abbreviations: ATR, anterior thalamic radiation; CCG, cingulum (cingulate gyrus); CH, cingulum (hippocampus); CST, corticospinal tract; FC, fiber cross section; FD, fiber density; FDC, FD and cross section; FDR, false discovery rate; FMaj, forceps major; FMin, forceps minor; IFOF, inferior fronto-occipital fasciculus; ILF, inferior longitudinal fasciculus; SLF, superior longitudinal fasciculus; SLTem, superior longitudinal fasciculus (temporal); UF, uncinate fasciculus.

corresponding increase in RD rather than in AD (Inano et al., 2011; Kumar et al., 2013). However, decreases in FA could not be driven entirely by myelin degeneration since diffusion anisotropy in WM fiber tracts could also be affected by several other microstructural features including axonal membrane, intra-axonal microstructure, as well as density and diameter of axons (Beaulieu, 2002; Paus, Pesaresi, & French, 2014; Takahashi et al., 2002). By using more direct measures of fiber bundle properties, we found widespread negative

correlation between FD and age. This finding is consistent with a postmortem study of the human brain investigating age-related changes in the corpus callosum which showed reduction in fiber number and density with selective degradation of small to medium caliber fibers, rather than demyelination, as important contributors to age-related WM atrophy (Hou & Pakkenberg, 2012). Similar significant reduction in small caliber myelinated fibers with age had also been reported in human (Tang, Nyengaard, Pakkenberg, &

Gundersen, 1997) as well as in rhesus monkey (Bowley, Cabral, Rosene, & Peters, 2010). In addition, we also observed that lower FD were particularly prominent in fiber bundles associated with the pre-frontal regions such as the cingulum of the cingulate gyrus and forceps minor, indicating greater vulnerability of these regions to aging effects. Studies using FA have also shown similar greater age-related reductions in FA in frontal regions relative to more posterior regions (Yoon, Shim, Lee, Shon, & Yang, 2008) consistent with our findings. Other studies have also provided evidence for this anterior-posterior gradient of age-related decreases in FA (Ardekani, Kumar, Bartzokis, & Sinha, 2007; Grieve, Williams, Paul, Clark, & Gordon, 2007). Together, our findings not only supported results from previous diffusion tensor imaging (DTI)-based studies but also provided greater specificity of the WM properties that were significantly affected by the aging process.

## 4.2 | Age-related alterations in FC across the whole brain

In contrast to FD, the FC of several WM fiber tracts appeared to be relatively preserved with age. This can be seen, for instance, in the corpus callosum fibers (Figure 3). With FD reduction, this relative preservation of FC in some fiber bundles could be indicative of an increase in the extra-axonal space left as more fibers degenerate. Alternatively, the extra-axonal space may also be persistently filled with other extracellular materials in spite of the axonal loss, thus preserving FC. For instance, electron micrograph of the cingulate bundle of aged rhesus monkey showed less tightly packed axonal myelinated nerve fibers than in younger monkeys, an indication of fiber loss, as well as cells related to astrocytic processes, dense cytoplasm in splits of myelin sheaths, and ballooning of the sheaths (Bowley et al., 2010). It is also interesting to note that this study also observed no significant change in cross-sectional area in the cingulate and corpus callosum with age.

Differences in caliber of the axons making up the fiber bundle could also influence the macrostructural changes in WM. As mentioned, since most of the axons affected by aging are of small caliber type (Bowley et al., 2010; Hou & Pakkenberg, 2012; Tang et al., 1997), FC of fiber bundles consisting of different caliber axons and those with large caliber axons would be minimally affected. This can be seen, for example, in the corpus callosum, which contains different classes of axons (from small to very large caliber axons) distributed in a region-specific manner (Lamantia & Rakic, 1990). The observed increase in mean fiber diameter with age (Hou & Pakkenberg, 2012; Tang et al., 1997) also points to the relative preservation of large caliber axons, which in turn may help in maintaining FC. These factors, among others, may have influenced the relative preservation of FC, although a more detailed microstructural study will be needed to clearly elucidate the relationship between FC and aging.

Higher values of FC in specific fiber bundles with advanced age, such as the one observed in the anterior thalamic radiation and tracts

connecting the hippocampus to the cingulum, are somewhat difficult to explain. Examples of regional preservation or even volumetric increases in specific brain regions in old age do exist. Recent meta-analysis demonstrated that aerobic exercise interventions may be useful for preventing age-related hippocampal deterioration (Firth et al., 2018). Exercise may also increase the level of the brain-derived neurotrophic factor (BDNF) (Szuhany, Bugatti, & Otto, 2015), positively linked with exercise-induced increase in hippocampal volume (Erickson et al., 2011). The effect of exercise in WM structure is still unclear (Sexton et al., 2016). Some evidences do indicate that life-long exercise may help preserved the microstructural integrity of WM fibers (Tseng et al., 2013). Unfortunately, we did not investigate the detailed exercise information from our participants but the effect of BDNF and exercise may have influenced the relatively higher FC values observed in the cingulum of the hippocampus in the elderly. We do note that the higher FC values in these tracts were not associated with higher FD values. In fact, these tracts' FD values were significantly lower in the elderly compared to young participants resulting in an overall lower FDC.

## 4.3 | Sex differences

Findings related to differences in sex with regard to WM aging are still inconsistent. Some studies reported no significant interaction between age and sex in WM aging process (Hsu et al., 2010; Inano et al., 2011), while others showed the contrary (Abe et al., 2010; Kumar et al., 2013). Using AD and RD, for instance, Kumar et al. (2013) have shown that females had reduced axonal and myelin integrity in substantially more structure, while males had reduced fiber and myelin integrity in only a minority of structures confined to cerebellar, temporal, and frontal cortices. In another study, males also showed steeper FA decline and accelerated MD increases with age in multiple brain regions compared with females, whereas no areas showed similar pattern in females compared with males (Abe et al., 2010).

Although the estimated mean FC and FDC values tended to be relatively higher in males than in females, our findings showed no significant sex differences in FBA metrics in most major fiber tract groups after taking into account variations in brain sizes. We did observe significant association between FC and FDC values with TIV suggesting that these macroscopic metrics could be strongly influenced by differences in brain sizes. Studies have shown that males have larger global WM volumes than females (Abe et al., 2010; Lemaitre et al., 2005). Even in terms of myelinated fibers, males were found to have 16% longer total fiber length than females (Marnier, Nyengaard, Tang, & Pakkenberg, 2003). Thus, it is not surprising that the estimated FC values were higher in males than in females. By including TIV as a covariate, differences in brain sizes between males and females could be statistically taken into account. However, we did observe that the coefficients associated with age in FD tended to be lower (more negative) in male participants than in females even after accounting for the differences in brain sizes.

## 4.4 | Limitations

For better estimates of the FOD and apparent FD (AFD), MRtrix3 recommends that DWI data be acquired with  $b$ -values of  $\sim 3,000$  s/mm<sup>2</sup>. Data acquired with multiple shells will also improve the accuracy of the estimation of the multitissue response functions and will result in more robust FOD and AFD estimates. One limitation of our study is the acquisition of DWI images at a single and relatively low  $b$ -value ( $b = 1,000$  S/mm<sup>2</sup>). While the imaging parameters still permit analysis, these are not ideal imaging conditions, which could lead to less accurate computation of the multitissue response functions. Although, in terms of test–retest reliability, a recent study has shown good reliability of the estimated three tissue compartments even for a single shell data ( $b = 1,500$  s/mm<sup>2</sup>) using a relatively different approach (Newman, Dhollander, Reynier, Panzer, & Druzgal, in press). At lower  $b$ -values, Raffelt et al. (2012) also argued that fiber orientations will not be compromised but AFD will possibly be overestimated in GM and CSF tissue (Jeurissen et al., 2014) and could also show larger dependency on extra-axonal perpendicular diffusivity which could potentially camouflage changes in the true underlying FD (Genc et al., 2020). Another limitation of the study is the unbalance number of male and female participants in our cohort. Although we strived to recruit equal number of both sexes, most of our participants were females, which could be a reflection of the overall ratio of men and women in the general population given the longer average life expectancy of women (87.26 years) as compared to men (81.09 years) in Japan. The higher stroke prevalence in men also led to the higher number of excluded male participants compared to females.

## 5 | CONCLUSION

Using DWI data from a cohort of 293 healthy volunteers, we found widespread and significant age-related changes in WM across the whole brain over the adult lifespan. The observed effect was non-uniform across WM with some fibers exhibiting higher vulnerability than the others. Differences in mean FC and FDC values between sexes were mostly explained by differences in brain sizes although male participants tended to exhibit steeper negative relationship with age in FD values than female participants. Overall, these findings corroborate results from previous DTI studies, are consistent with post-mortem observations of the aging brain, and further demonstrate the usefulness of diffusion imaging in the study of microstructural age-related changes in the brain's WM.

### ACKNOWLEDGMENTS

This work was supported by Grants-in-Aid from the Research Committee of Central Nervous System Degenerative Diseases by the Ministry of Health, Labor, and Welfare and from the Integrated Research on Neuropsychiatric Disorders project carried out under the Strategic Research for Brain Sciences by the Ministry of Education, Culture, Sports, Science, and Technology (MEXT) of Japan. This work was also supported by a Grant-in-Aid for Scientific Research from MEXT, Japan

(grant number: 80569781), and a Grant-in-Aid for Scientific Research on Innovative Areas (Brain Protein Aging and Dementia Control) (grant number: 26117002) also from MEXT. Analysis of the data was performed in collaboration with the Center of Intelligent Signal and Imaging Research (CISIR), Universiti Teknologi PETRONAS, Malaysia, which acknowledges support from the Ministry of Higher Education Malaysia HI-CoE Program. The funders had no role in study design, data collection and analysis, decision to publish, or preparation of the manuscript. The authors declare no conflict of interest with regard to this submission.

### CONFLICT OF INTEREST

The authors declare no potential conflict of interest.

### DATA AVAILABILITY STATEMENT

The data generated and analyzed in this study are not publicly available due to privacy and ethical restrictions. Requests for data can be made to the corresponding author and will be subject to approval from the Ethics Committee of Nagoya University Graduate School of Medicine.

### ORCID

Shao Wei Choy  <https://orcid.org/0000-0001-6855-3670>

Epifanio Bagarinao  <https://orcid.org/0000-0001-5000-6943>

Gen Sobue  <https://orcid.org/0000-0003-4769-5922>

### REFERENCES

- Abe, O., Yamasue, H., Yamada, H., Masutani, Y., Kabasawa, H., Sasaki, H., ... Ohtomo, K. (2010). Sex dimorphism in gray/white matter volume and diffusion tensor during normal aging. *NMR in Biomedicine*, 23, 446–458.
- Allen, J. S., Bruss, J., Brown, C. K., & Damasio, H. (2005). Normal neuroanatomical variation due to age: The major lobes and a parcellation of the temporal region. *Neurobiology of Aging*, 26, 1245–1260.
- Andersson, J. L. R., & Sotiropoulos, S. N. (2016). An integrated approach to correction for off-resonance effects and subject movement in diffusion MR imaging. *NeuroImage*, 125, 1063–1078.
- Ardekani, S., Kumar, A., Bartzokis, G., & Sinha, U. (2007). Exploratory voxel-based analysis of diffusion indices and hemispheric asymmetry in normal aging. *Magnetic Resonance Imaging*, 25, 154–167.
- Avants, B. B., Tustison, N. J., Stauffer, M., Song, G., Wu, B., & Gee, J. C. (2014). The insight ToolKit image registration framework. *Frontiers in Neuroinformatics*, 8, 44 Retrieved from <http://journal.frontiersin.org/article/10.3389/fninf.2014.00044/abstract>
- Bagarinao, E., Watanabe, H., Maesawa, S., Mori, D., Hara, K., Kawabata, K., ... Sobue, G. (2019). Reorganization of brain networks and its association with general cognitive performance over the adult lifespan. *Scientific Reports*, 9, 11352 Retrieved from <http://www.nature.com/articles/s41598-019-47922-x>
- Bagarinao, E., Watanabe, H., Maesawa, S., Mori, D., Hara, K., Kawabata, K., ... Sobue, G. (2018). An unbiased data-driven age-related structural brain parcellation for the identification of intrinsic brain volume changes over the adult lifespan. *NeuroImage*, 169, 134–144 Retrieved from <http://linkinghub.elsevier.com/retrieve/pii/S1053811917310285>
- Beaulieu, C. (2002). The basis of anisotropic water diffusion in the nervous system—A technical review. *NMR in Biomedicine*, 15, 435–455.
- Beck, A. T., Ward, C. H., Mendelson, M., Mock, J., & Erbaugh, J. (1961). Beck depression inventory. *Archives of General Psychiatry*, 4, 561–571 Retrieved from <http://www.ncbi.nlm.nih.gov/pubmed/21441403>

- Bennett, I. J., & Madden, D. J. (2014). Disconnected aging: Cerebral white matter integrity and age-related differences in cognition. *Neuroscience*, 276, 187–205.
- Bowley, M. P., Cabral, H., Rosene, D. L., & Peters, A. (2010). Age changes in myelinated nerve fibers of the cingulate bundle and corpus callosum in the rhesus monkey. *The Journal of Comparative Neurology*, 518, 3046–3064.
- Cox, S. R., Ritchie, S. J., Tucker-Drob, E. M., Liewald, D. C., Hagenaars, S. P., Davies, G., ... Deary, I. J. (2016). Ageing and brain white matter structure in 3,513 UK Biobank participants. *Nature Communications*, 7, 13629.
- dos Santos Kawata, K. H., Hashimoto, R., Nishio, Y., Hayashi, A., Ogawa, N., Kanno, S., ... Mori, E. (2012). A validation study of the Japanese version of the Addenbrooke's cognitive examination-revised. *Dementia and Geriatric Cognitive Disorders Extra*, 2, 29–37.
- Erickson, K. I., Voss, M. W., Prakash, R. S., Basak, C., Szabo, A., Chaddock, L., ... Kramer, A. F. (2011). Exercise training increases size of hippocampus and improves memory. *Proceedings of the National Academy of Sciences of the United States of America*, 108, 3017–3022.
- Firth, J., Stubbs, B., Vancampfort, D., Schuch, F., Lagopoulos, J., Rosenbaum, S., & Ward, P. B. (2018). Effect of aerobic exercise on hippocampal volume in humans: A systematic review and meta-analysis. *NeuroImage*, 166, 230–238.
- Fjell, A. M., Westlye, L. T., Grydeland, H., Amlie, I., Espeseth, T., Reinvang, I., ... Walhovd, K. B. (2013). Critical ages in the life course of the adult brain: Nonlinear subcortical aging. *Neurobiology of Aging*, 34, 2239–2247.
- Gajamange, S., Raffelt, D., Dhollander, T., Lui, E., van der Walt, A., Kilpatrick, T., ... Kolbe, S. (2018). Fibre-specific white matter changes in multiple sclerosis patients with optic neuritis. *NeuroImage: Clinical*, 17, 60–68.
- Genc, S., Smith, R. E., Malpas, C. B., Anderson, V., Nicholson, J. M., Efron, D., ... Silk, T. J. (2018). Development of white matter fibre density and morphology over childhood: A longitudinal fixel-based analysis. *NeuroImage*, 183, 666–676.
- Genc, S., Tax, C. M. W., Raven, E. P., Chamberland, M., Parker, G. D., & Jones, D. K. (2020). Impact of b-value on estimates of apparent fibre density. *bioRxiv*. <https://doi.org/10.1101/2020.01.15.905802>
- Good, C. D., Johnsru, I. S., Ashburner, J., Henson, R. N. A., Friston, K. J., & Frackowiak, R. S. J. (2001). A voxel-based morphometric study of ageing in 465 normal adult human brains. *NeuroImage*, 14, 21–36 Retrieved from <http://linkinghub.elsevier.com/retrieve/pii/S1053811901907864%5Cnhttp://www.ncbi.nlm.nih.gov/pubmed/11525331>
- Greenberg, D. L., Messer, D. F., Payne, M. E., MacFall, J. R., Provenzale, J. M., Steffens, D. C., & Krishnan, R. R. (2008). Aging, gender, and the elderly adult brain: An examination of analytical strategies. *Neurobiology of Aging*, 29, 290–302.
- Grieve, S. M., Williams, L. M., Paul, R. H., Clark, C. R., & Gordon, E. (2007). Cognitive aging, executive function, and fractional anisotropy: A diffusion tensor MR imaging study. *American Journal of Neuroradiology*, 28, 226–235.
- Hou, J., & Pakkenberg, B. (2012). Age-related degeneration of corpus callosum in the 90+ years measured with stereology. *Neurobiology of Aging*, 33, 1009.e1–1009.e9.
- Hsu, J. L., van Hecke, W., Bai, C. H., Lee, C. H., Tsai, Y. F., Chiu, H. C., ... Leemans, A. (2010). Microstructural white matter changes in normal aging: A diffusion tensor imaging study with higher-order polynomial regression models. *NeuroImage*, 49, 32–43.
- Hua, K., Zhang, J., Wakana, S., Jiang, H., Li, X., Reich, D. S., ... Mori, S. (2008). Tract probability maps in stereotaxic spaces: Analyses of white matter anatomy and tract-specific quantification. *NeuroImage*, 39, 336–347.
- Inano, S., Takao, H., Hayashi, N., Abe, O., & Ohtomo, K. (2011). Effects of age and gender on white matter integrity. *American Journal of Neuroradiology*, 32, 2103–2109.
- Jenkinson, M., Beckmann, C. F., Behrens, T. E. J., Woolrich, M. W., & Smith, S. M. (2012). FSL. *NeuroImage*, 62, 782–790.
- Jernigan, T. L., Archibald, S. L., Fennema-Notestine, C., Gamst, A. C., Stout, J. C., Bonner, J., & Hesselink, J. R. (2001). Effects of age on tissues and regions of the cerebrum and cerebellum. *Neurobiology of Aging*, 22, 581–594.
- Jeurissen, B., Tournier, J. D., Dhollander, T., Connelly, A., & Sijbers, J. (2014). Multi-tissue constrained spherical deconvolution for improved analysis of multi-shell diffusion MRI data. *NeuroImage*, 103, 411–426.
- Kumar, R., Chavez, A. S., Macey, P. M., Woo, M. A., & Harper, R. M. (2013). Brain axial and radial diffusivity changes with age and gender in healthy adults. *Brain Research*, 1512, 22–36.
- Lamantia, A. -S., & Rakic, P. (1990). Cytological and quantitative characteristics of four cerebral commissures in the rhesus monkey. *The Journal of Comparative Neurology*, 291, 520–537.
- Lebel, C., Gee, M., Camicioli, R., Wieler, M., Martin, W., & Beaulieu, C. (2012). Diffusion tensor imaging of white matter tract evolution over the lifespan. *NeuroImage*, 60, 340–352.
- Lemaître, H., Crivello, F., Grassiot, B., Alperovitch, A., Tzourio, C., & Mazoyer, B. (2005). Age- and sex-related effects on the neuroanatomy of healthy elderly. *NeuroImage*, 26, 900–911.
- Marnier, L., Nyengaard, J. R., Tang, Y., & Pakkenberg, B. (2003). Marked loss of myelinated nerve fibers in the human brain with age. *The Journal of Comparative Neurology*, 462, 144–152.
- Mioshi, E., Dawson, K., Mitchell, J., Arnold, R., & Hodges, J. R. (2006). The Addenbrooke's cognitive examination revised (ACE-R): A brief cognitive test battery for dementia screening. *International Journal of Geriatric Psychiatry*, 21, 1078–1085.
- Mito, R., Raffelt, D., Dhollander, T., Vaughan, D. N., Tournier, J. D., Salvado, O., ... Connelly, A. (2018). Fibre-specific white matter reductions in Alzheimer's disease and mild cognitive impairment. *Brain*, 141, 888–902.
- Mugler, J. P., & Brookeman, J. R. (1990). Three-dimensional magnetization-prepared rapid gradient-echo imaging (3D MP RAGE). *Magnetic Resonance in Medicine*, 15, 152–157. <http://www.ncbi.nlm.nih.gov/pubmed/2374495>
- Newman, B. T., Dhollander, T., Reynier, K. A., Panzer, M. B., & Druzgal, T. J. (in press). Test-retest reliability and long-term stability of three-tissue constrained spherical deconvolution methods for analyzing diffusion MRI data. *Magnetic Resonance in Medicine*. <https://doi.org/10.1002/mrm.28242>
- Paus, T., Pesaresi, M., & French, L. (2014). White matter as a transport system. *Neuroscience*, 276, 117–125.
- Raffelt, D., Tournier, J.-D. D., Rose, S., Ridgway, G. R., Henderson, R., Crozier, S., ... Connelly, A. (2012). Apparent fibre density: A novel measure for the analysis of diffusion-weighted magnetic resonance images. *NeuroImage*, 59, 3976–3994.
- Raffelt, D. A., Smith, R. E., Ridgway, G. R., Tournier, J. D., Vaughan, D. N., Rose, S., ... Connelly, A. (2015). Connectivity-based fixel enhancement: Whole-brain statistical analysis of diffusion MRI measures in the presence of crossing fibres. *NeuroImage*, 117, 40–55.
- Raffelt, D. A., Tournier, J. D., Smith, R. E., Vaughan, D. N., Jackson, G., Ridgway, G. R., & Connelly, A. (2017). Investigating white matter fibre density and morphology using fixel-based analysis. *NeuroImage*, 144, 58–73.
- Ryali, S., Glover, G. H., Chang, C., & Menon, V. (2009). Development, validation, and comparison of ICA-based gradient artifact reduction algorithms for simultaneous EEG-spiral in/out and echo-planar fMRI recordings. *NeuroImage*, 48, 348–361.
- Sala, S., Agosta, F., Pagani, E., Copetti, M., Comi, G., & Filippi, M. (2012). Microstructural changes and atrophy in brain white matter tracts with aging. *Neurobiology of Aging*, 33, 488–498.
- Salat, D. H., Tuch, D. S., Greve, D. N., van der Kouwe, A. J. W., Hevelone, N. D., Zaleta, A. K., ... Dale, A. M. (2005). Age-related

- alterations in white matter microstructure measured by diffusion tensor imaging. *Neurobiology of Aging*, 26, 1215–1227.
- Sexton, C. E., Betts, J. F., Demnitz, N., Dawes, H., Ebmeier, K. P., & Johansen-Berg, H. (2016). A systematic review of MRI studies examining the relationship between physical fitness and activity and the white matter of the ageing brain. *NeuroImage*, 131, 81–90.
- Smith, C. D., Chebrolu, H., Wekstein, D. R., Schmitt, F. A., & Markesbery, W. R. (2007). Age and gender effects on human brain anatomy: A voxel-based morphometric study in healthy elderly. *Neurobiology of Aging*, 28, 1075–1087.
- Smith, R. E., Tournier, J.-D., Calamante, F., & Connelly, A. (2013). SIFT: Spherical-deconvolution informed filtering of tractograms. *NeuroImage*, 67, 298–312.
- Smith, S. M., Jenkinson, M., Woolrich, M. W., Beckmann, C. F., Behrens, T. E. J., Johansen-Berg, H., ... Matthews, P. M. (2004). Advances in functional and structural MR image analysis and implementation as FSL. *NeuroImage*, 23, S208–S219.
- Song, S. K., Sun, S. W., Ju, W. K., Lin, S. J., Cross, A. H., & Neufeld, A. H. (2003). Diffusion tensor imaging detects and differentiates axon and myelin degeneration in mouse optic nerve after retinal ischemia. *NeuroImage*, 20, 1714–1722.
- Song, S. K., Yoshino, J., Le, T. Q., Lin, S. J., Sun, S. W., Cross, A. H., & Armstrong, R. C. (2005). Demyelination increases radial diffusivity in corpus callosum of mouse brain. *NeuroImage*, 26, 132–140.
- Sullivan, E. V., & Pfefferbaum, A. (2006). Diffusion tensor imaging and aging. *Neuroscience and Biobehavioral Reviews*, 30, 749–761.
- Szuhany, K. L., Bugatti, M., & Otto, M. W. (2015). A meta-analytic review of the effects of exercise on brain-derived neurotrophic factor. *Journal of Psychiatric Research*, 60, 56–64.
- Takahashi, M., Hackney, D. B., Zhang, G., Wehrli, S. L., Wright, A. C., O'Brien, W. T., ... Selzer, M. E. (2002). Magnetic resonance micro-imaging of intraaxonal water diffusion in live excised lamprey spinal cord. *Proceedings of the National Academy of Sciences of the United States of America*, 99, 16192–16196.
- Taki, Y., Goto, R., Evans, A., Zijdenbos, A., Neelin, P., Lerch, J., ... Fukuda, H. (2004). Voxel-based morphometry of human brain with age and cerebrovascular risk factors. *Neurobiology of Aging*, 25, 455–463.
- Taki, Y., Thyreau, B., Kinomura, S., Sato, K., Goto, R., Kawashima, R., & Fukuda, H. (2011). Correlations among brain gray matter volumes, age, gender, and hemisphere in healthy individuals. *PLoS One*, 6, e22734.
- Tang, Y., Nyengaard, J. R., Pakkenberg, B., & Gundersen, H. J. G. (1997). Age-induced white matter changes in the human brain: A stereological investigation. *Neurobiology of Aging*, 18, 609–615.
- Tournier, J.-D., Calamante, F., Connelly, A. (2010). Improved probabilistic streamlines tractography by 2nd order integration over fibre orientation distributions. In: *Proceedings of the International Society for Magnetic Resonance in Medicine*; 1670.
- Tournier, J.-D., Mori, S., & Leemans, A. (2011). Diffusion tensor imaging and beyond. *Magnetic Resonance in Medicine*, 65, 1532–1556.
- Tseng, B. Y., Gundapuneedi, T., Khan, M. A., Diaz-Arrastia, R., Levine, B. D., Lu, H., ... Zhang, R. (2013). White matter integrity in physically fit older adults. *NeuroImage*, 82, 510–516.
- Yoon, B., Shim, Y. S., Lee, K. S., Shon, Y. M., & Yang, D. W. (2008). Region-specific changes of cerebral white matter during normal aging: A diffusion-tensor analysis. *Archives of Gerontology and Geriatrics*, 47, 129–138.

## SUPPORTING INFORMATION

Additional supporting information may be found online in the Supporting Information section at the end of this article.

**How to cite this article:** Choy SW, Bagarinao E, Watanabe H, et al. Changes in white matter fiber density and morphology across the adult lifespan: A cross-sectional fixel-based analysis. *Hum Brain Mapp*. 2020;41:3198–3211. <https://doi.org/10.1002/hbm.25008>